

Figure S1. Ciliary loss of Gpr161 depends on its signaling activity and direct binding to β -arrestins. (A) Stable T-REx-293 cells expressing CAMYEL (conformation-based cAMP BRET biosensor) and inducibly coexpressing untagged mouse *Gpr161* were treated with 4 μ g/ml doxycycline (Dox) for 12 h. The media was replaced with assay buffer containing 1 mM IBMX 45 min before the experiment. Readings were taken using 475- and 535-nm emission filters simultaneously after the addition of 5 μ M coelenterazine-h. After tracking the baseline BRET ratio for 2 min, cells were treated with drugs (10 μ M each) or 10 μ M Forskolin using injectors (indicated by arrow). Oxysterols used were as follows: 7-keto-27-hydroxycholesterol, a naturally occurring oxysterol (Myers et al., 2013), 20 α -hydroxycholesterol, a synthetic oxysterol (Nachtergaele et al., 2012), and 7 α ,25-dihydroxycholesterol, which is an agonist for Gpr183 (Hannedouche et al., 2011). The BRET ratios were subsequently quantified for 5 min. Mean values of two independent experiments are represented graphically. (B) Confluent NIH 3T3 Flp-In cells stably expressing GFP-tagged WT *Gpr161* were starved for a total of 24 h and treated with SAG (500 nM) for indicated time periods before fixation. Fixed cells were processed for immunofluorescence with anti-GFP and anti-acetylated tubulin antibodies, for detecting GFP-positive cilia. Data represents mean \pm SD from two experiments. (C and D) Confluent NIH 3T3 Flp-In cells stably expressing GFP-tagged full-length *Gpr161* V158E mutant (VE) were starved \pm 1 μ M SAG for 24 h, and Gpr161 (C) and Smo (D) levels in cilia were determined by immunofluorescence. For C, GFP ciliary intensities in cilia were quantified using ImageJ ($n = 50$ each; *, $P < 0.01$). For D, data represent mean \pm SD from three separate fields from one experiment (*, $P < 0.001$ with respect to untreated cells in each cell line). (E) Confluent NIH 3T3 Flp-In cells stably expressing indicated constructs were starved for 30 h, and immunoblotted for indicated proteins (Materials and methods). Relative transcript levels for *Gpr161*^{GFP} were determined in parallel by qRT-PCR (mean \pm SD). (F) Confluent IMCD3 Flp-In cells were starved for 24 h and treated with \pm 250 nM SAG for the last 90 min. β -arrestin localization to cilia is shown after immunofluorescence with anti-pan- β -arrestin and acetylated tubulin (AcTub) antibodies. Bar, 5 μ m. (G and H) Confluent WT and β -arrestin 1/2 double-knockout MEFs (*Arrb1/2* dko) were starved for 48 h, treated with 500 nM SAG for the indicated time points before fixation, and processed for immunofluorescence using anti-Gpr161 and anti-acetylated tubulin antibodies to quantify cilia positive for Gpr161 by microscopy. Data represent mean \pm SD from three independent experiments. *, $P < 0.001$, with respect to untreated WT cells. (I) Confluent NIH 3T3 Flp-In cells stably expressing GFP-tagged *Gpr161*^{Δ376} mutant were starved for 24 h \pm 1 μ M SAG before fixation, and immunostained using anti-GFP/anti-Smo and anti-acetylated tubulin antibodies. Data represent mean \pm SD from two independent experiments for Gpr161 IF, and three separate fields from one experiment for Smo IF. *, $P < 0.001$ with respect to untreated cells.

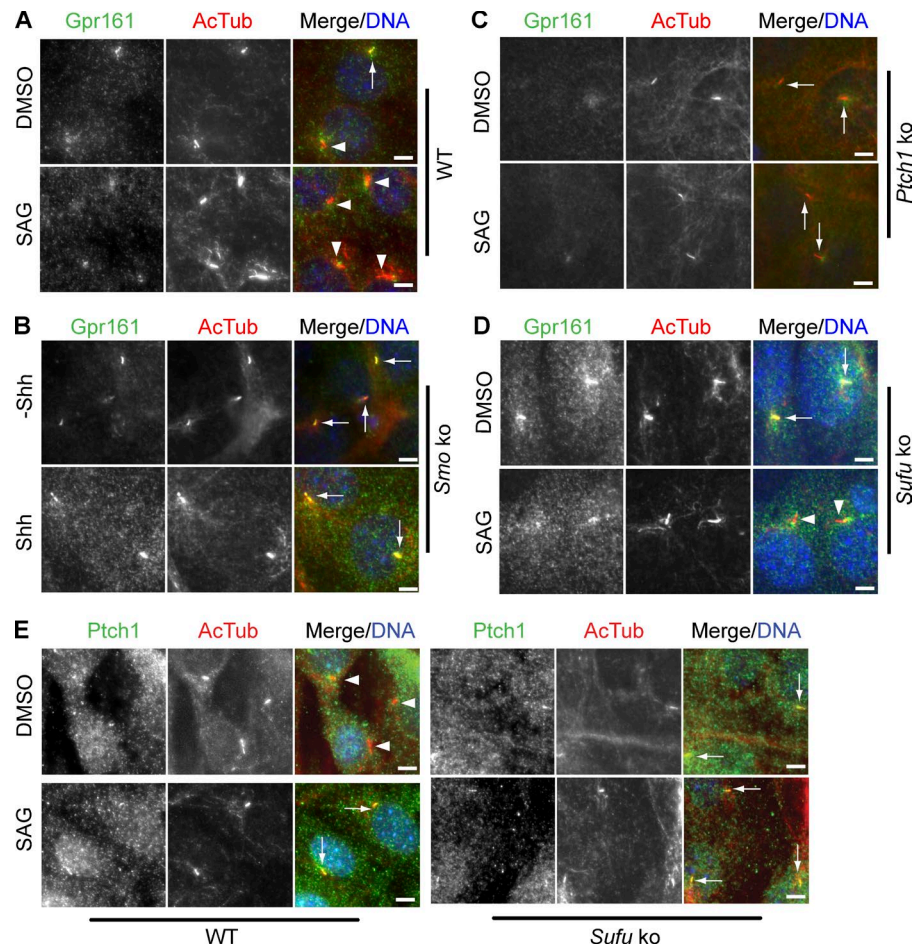


Figure S2. **Steady-state localization of Gpr161 in cilia is not controlled by Shh pathway activity.** (A–D) Confluent WT, *Smo*^{-/-}, *Ptch1*^{-/-}, or *Sufu*^{-/-} MEFs were serum starved for 48 h, treated with 500 nM SAG or 300 ng/ml octyl-Shh for the last 24 h before fixation, and immunostained using anti-Gpr161 (green) and anti-acetylated tubulin (AcTub; red) antibodies. Bar, 5 μm. (E) Confluent WT and *Sufu*^{-/-} MEFs were serum starved for 48 h, treated with 500 nM SAG for the last 24 h before fixation, and immunostained using anti-Ptch1 (green) and anti-acetylated tubulin (AcTub; red) antibodies. Bar, 5 μm.

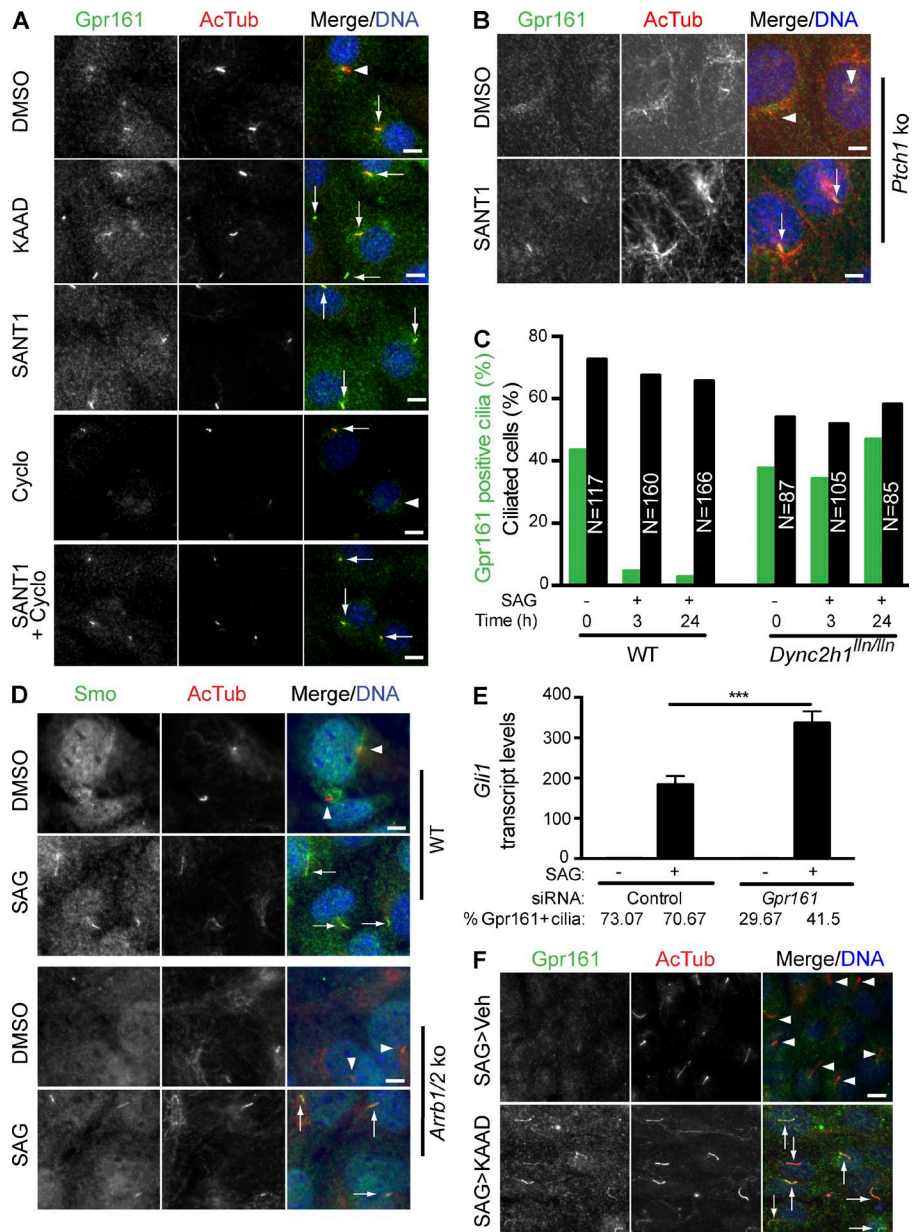


Figure S3. Presence of activated Smo in cilia determines steady-state levels of Gpr161. (A) Confluent WT MEFs were serum starved for 48 h, treated with drugs for last 24 h before fixation, and immunostained for Gpr161 (green) and acetylated tubulin (AcTub; red). Drugs used were as follows: 500 nM SAG, 1 μ M KAAD-cyclopamine (KAAD), 1 μ M GDC-0449 (GDC), 1 μ M SANT1, and 5 μ M cyclopamine (cyclo). Arrows and arrowheads indicate cilia positive and negative for Gpr161, respectively. Bar, 5 μ m. (B) Confluent *Ptch1*^{-/-} MEFs were serum starved for 48 h, treated \pm 1 μ M SANT1 for the last 24 h before fixation, and immunostained using anti-Gpr161 (green) and anti-acetylated tubulin (AcTub; red) antibodies. Bar, 5 μ m. (C) Confluent WT and *Dync2h1*^{fln/fln} MEFs (Ocbina et al., 2011) were serum starved for 48 h, treated \pm 500 nM SAG for the indicated time periods before fixation, and immunostained using anti-Gpr161 (green) and anti-acetylated tubulin (red) antibodies to quantify Gpr161-positive cilia. N, total counted cilia from one experiment. (D) Confluent WT and *β -arrestin1/2* double-knockout MEFs (*Arrb1/2 ko*) were serum starved for 48 h, treated \pm 1 μ M SAG in starvation media for 36 h before fixation, and immunostained using anti-Smo (green) and anti-acetylated tubulin (AcTub; red) antibodies. Arrows and arrowheads indicate cilia positive and negative for Smo, respectively. (E) *β -arrestin1/2* double-knockout MEFs were transfected with siRNAs against *Gpr161* (Materials and methods). Confluent cells were starved for 24 h and further treated \pm 1 μ M SAG for 30 h in starvation media. Total RNA was isolated, and *Gli1* expression levels were determined by quantitative real-time RT-PCR. Percentages of Gpr161-positive cilia upon RNAi suggests partial knockdown of the receptor in the primary MEFs. Data represent mean \pm SEM from three independent experiments. ***, $P < 0.001$. (F) SAG-pretreated IMCD3 cells \pm KAAD-cyclopamine, as described in Fig. 3 F, were immunostained to detect ciliary Gpr161 levels. Arrowheads and arrows indicate cilia negative and positive for Gpr161, respectively. Bar, 10 μ m.

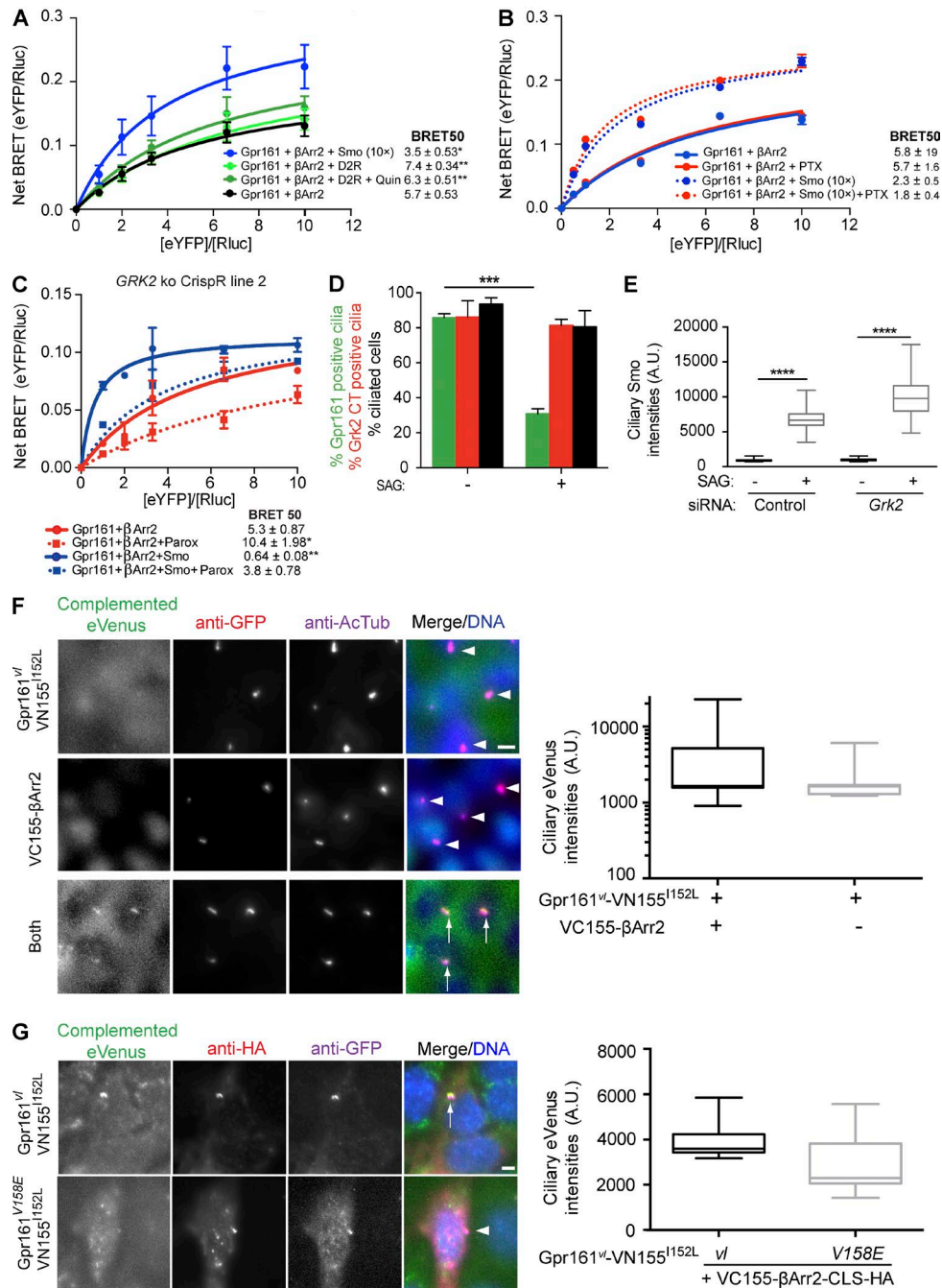


Figure S4. Smo enhances recruitment of β-Arrestin to Gpr161. (A and B) T-REx 293 cells were cotransfected with a constant amount of Rluc-β-arrestin1/2 (donor) and increasing amounts of Gpr161-eYFP (acceptor), ±1 μg/well of a six-well plate untagged human Smo (10x), ±1 μg/well of a six-well plate Flag-D2R. Flag-D2R-transfected cells were also finally treated with 1 μM of the D2R agonist quinirole for 20 min (A). The cells were incubated with 800 ng/ml pertussis toxin for 12 h before the BRET assays (B). Cells were subjected to BRET analysis (Materials and methods). The titration curves are mean ± SEM from three independent experiments (A) and mean ± SD from one experiment performed in duplicate (B). *, P < 0.05; **, P < 0.01 for BRET₅₀ values with respect to only Gpr161/β-arrestin2 cotransfected cells in A. (C) BRET assays for Gpr161-β-arrestin2 interactions as in Fig. 5 C with GRK2 knockout line 2 from two independent experiments (mean ± SD). *, P < 0.05; **, P < 0.01 with respect to Rluc-β-arrestin2 binding to Gpr161-eYFP. (D) IMCD3 cells transfected with ciliary-targeted Grk2 C-terminus fusion (CLS-mCherry-Grk2CT; Materials and methods) were starved ±500 nM SAG for 17 h and subjected to immunofluorescence for Gpr161 (green) and anti-acetylated tubulin (magenta). CLS-mCherry-Grk2CT positive (red) cilia were scored for Gpr161. Data represents mean ± SD from two experiments. ***, P < 0.001. (E) Pixel intensities of Smo in control or *Grk2* siRNA-treated IMCD3 cilia ± SAG treatment represented graphically. n = 100 each; ****, P < 0.0001 with respect to untreated cells in each background. (F) IMCD3 cells with stable expression of Gpr161^{vl}-VN155^{I152L} were infected ± retroviruses expressing VC155-βArr2. After antibiotic selection, confluent cells were starved for 24 h before fixing and immunostained with anti-GFP (red) anti-acetylated tubulin (AcTub; magenta) antibodies. Intensities of eVenus complementation in the cilia (green channel) of GFP-positive cells (red channel) were quantified using ImageJ and represented graphically (right); n = 21 each. Bar, 5 μm. (G) IMCD3 cells were transfected with the indicated constructs (Materials and methods), starved for 17 h before fixing, and immunostained with anti-HA (red) anti-GFP (magenta) antibodies. Intensities of eVenus complementation in the cilia (green channel) of HA/GFP-positive cells were quantified using ImageJ and represented graphically (right); n ≥ 22 each. Bar, 5 μm. P < 0.001 between groups. Arrows and arrowheads indicate cilia positive and negative for eVenus complementation, respectively (F and G).

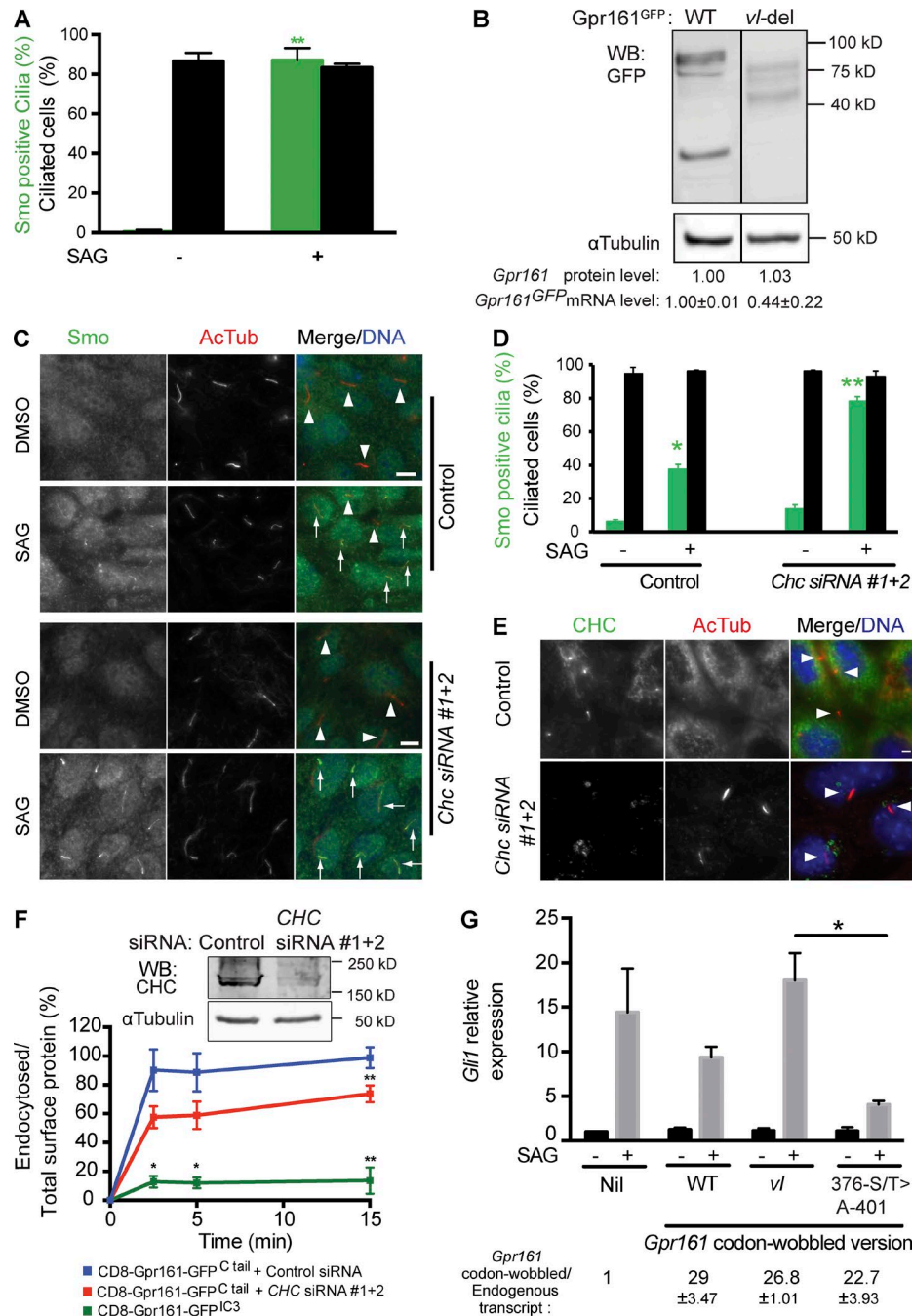


Figure S5. **Disappearance of Gpr161 from cilia is dependent on clathrin-mediated endocytosis.** (A) Confluent NIH 3T3 Flp-In cells stably expressing GFP-tagged *Gpr161^{vl}* mutant were treated $\pm 1 \mu\text{M}$ SAG for 24 h in starvation media before fixation, and Smo levels were quantified by immunofluorescence. Data represent mean \pm SD from three separate fields from one experiment. **, $P < 0.01$ with respect to untreated cells. (B) Confluent NIH 3T3 Flp-In cells stably transfected with indicated constructs were starved for 30 h and immunoblotted for indicated proteins (Materials and methods). Relative transcript levels for *Gpr161^{GFP}* were determined in parallel by quantitative real-time RT-PCR (mean \pm SD). (C and D) IMCD3 Flp-In cells were transfected with predesigned On-target Plus siRNAs against clathrin heavy chain (*Chc*) for 72 h. Confluent cells were starved for 30 h, treated $\pm 250 \text{ nM}$ SAG for 5 h before fixing, and immunostained using anti-Smo (green) and anti-acetylated tubulin (AcTub; red) antibodies to quantify cilia positive for Smo. Arrows and arrowheads indicate cilia positive and negative for Smo, respectively. Bar, 10 μm . Data represent mean \pm SD from three separate fields from one experiment. *, $P < 0.001$; **, $P < 0.0001$ with respect to DMSO-treated cells in each case. (E) IMCD3 Flp-In cells transfected with indicated predesigned siRNAs for 72 h were starved for the last 24 h, fixed, and immunostained for CHC. *Chc* siRNA-treated cells show specificity of the anti-CHC antibody. Arrowheads denote cilia. Bar, 5 μm . (F) ARPE-19 cells reverse transfected with siRNAs against *CHC* were transfected with plasmids expressing CD8 α -tagged with Gpr161 C tail or third intracellular loop (IC3) fragments (Materials and methods) the next day. Cells were subjected to ELISA (Materials and methods). Endocytosed CD8 α fusion proteins were expressed as a percentage of surface CD8 fusions. Inset shows immunoblot for *CHC*. Data represent mean \pm SEM from three experiments. *, $P < 0.05$; **, $P < 0.01$ with respect to control siRNA-treated cells at respective time points. (G) Confluent NIH 3T3 cells stably expressing untagged codon-wobbled wild type or mutant *Gpr161* (Materials and methods) were treated \pm SAG in starvation media for 30 h, followed by RNA isolation and quantification of *Gli1* levels by quantitative real-time RT-PCR. Data represent mean \pm SEM from three separate stable lines in each background and one to four independent experiments for each line. Quantitative real-time RT-PCR confirmed *Gpr161* overexpression to be identical between the respective lines (Materials and methods). *, $P < 0.05$.

References

- Hannedouche, S., J. Zhang, T. Yi, W. Shen, D. Nguyen, J.P. Pereira, D. Guerini, B.U. Baumgarten, S. Roggo, B. Wen, et al.. 2011. Oxysterols direct immune cell migration via EBI2. *Nature*. 475:524–527. <http://dx.doi.org/10.1038/nature10280>
- Myers, B.R., N. Sever, Y.C. Chong, J. Kim, J.D. Belani, S. Rychnovsky, J.F. Bazan, and P.A. Beachy. 2013. Hedgehog pathway modulation by multiple lipid binding sites on the smoothed effector of signal response. *Dev. Cell*. 26:346–357. <http://dx.doi.org/10.1016/j.devcel.2013.07.015>
- Nachtergaele, S., L.K. Mydock, K. Krishnan, J. Rammohan, P.H. Schlesinger, D.F. Covey, and R. Rohatgi. 2012. Oxysterols are allosteric activators of the oncoprotein Smoothed. *Nat. Chem. Biol.* 8:211–220. <http://dx.doi.org/10.1038/nchembio.765>
- Ocbina, P.J., J.T. Eggenschwiler, I. Moskowitz, and K.V. Anderson. 2011. Complex interactions between genes controlling trafficking in primary cilia. *Nat. Genet.* 43:547–553. <http://dx.doi.org/10.1038/ng.832>